Fluid Geochemistry of High-Temperature Hydrothermal Fields in the Okinawa Trough

30

Shinsuke Kawagucci

Abstract

This review compiles fluid chemistries of the six known high-temperature hydrothermal fields in the Okinawa Trough (OT) and compares them to global representative fields with various tectonic/geologic backgrounds. The comparisons indicate that the chemical characteristics of the OT hydrothermal fluids are explained by linkages between (1) shallow water depth that constrains the maximum fluid temperature, (2) back-arc tectonic setting that introduces magmatic volatiles into the fluid, (3) probable silicic rock-based fluid-mineral interaction at the hydrothermal reaction zone, and (4) seafloor sediment around the vents that provides both compounds derived from sedimentary organic matter and biogenic compounds, such as methane, produced by microbial ecosystems in the sedimentary environment.

To explain the highly diverse gas compositions and stable isotope ratios of methane among the OT hydrothermal fields, "fluid-sediment interaction" has been further classified into several types with respect to processes (microbial or chemical) and stages of subseafloor fluid circulation (recharge or discharge). This concept, called the Microbial Methanogenesis at Recharge stage (MMR) model, enables us not only to deduce the geochemical origins of the hydrothermal fluid CH_4 in each OT field but also to estimate the geographical distribution of hydrothermal fluid circulation via a two-dimension schematic illustration. The model, which links the fluid geochemistry with the subseafloor fluid migration path, will serve as a base for future studies also for any subseafloor geofluid systems that include hydrothermal systems, subseafloor methane hydrate, and seismogenic fault zone.

Keywords

High-temperature hydrothermal fluid geochemistry • Inter-field comparison • Okinawa trough • Origin of methane

30.1 Introduction

Active hydrothermal systems in the Okinawa Trough (OT) are representative of one of the four TAIGAs, i.e., the 'TAIGA of Methane' (Urabe et al. Chap. 1). Numerous cruises for more than two decades have investigated the hydrothermal activities and fluid geochemistry of high-temperature hydrothermal fields within the OT, such as Minami-Ensei (Chiba et al. 1993; Kawagucci et al. 2013a), Iheya North (Nakagawa et al. 2005; Kawagucci et al. 2011,

S. Kawagucci (✉)
Institute of Biogeosciences (Biogeos), Japan Agency for Marine-Earth Science and Technology (JAMSTEC), 2-15 Natsushima-cho, Yokosuka, Kanagawa 237-0061, Japan

Precambrian Ecosystem Laboratory (PEL), Japan Agency for Marine-Earth Science and Technology (JAMSTEC), 2-15 Natsushima-cho, Yokosuka, Kanagawa 237-0061, Japan

Submarine Resources Research Project (SRRP), Japan Agency for Marine-Earth Science and Technology (JAMSTEC), 2-15 Natsushima-cho, Yokosuka, Kanagawa 237-0061, Japan
e-mail: kawagucci@jamstec.go.jp

J.-i. Ishibashi et al. (eds.), *Subseafloor Biosphere Linked to Hydrothermal Systems: TAIGA Concept*,
DOI 10.1007/978-4-431-54865-2_30, © The Author(s) 2015

2013b), Jade (Sakai et al. 1990a, 1990b; Ishibashi et al. 1995), Hakurei (Ishibashi et al. 2014), Hatoma (Nakano et al. 2001; Saegusa et al. 2006; Kawagucci et al. 2010b; Toki et al., in preparation), and Daiyon-Yonaguni (Yonaguni IV) (Kishida et al. 2004; Konno et al. 2006; Suzuki et al. 2008). The most notable characteristics of the fluid chemistry of the OT hydrothermal fields are abundant millimolar levels of CH_4 (Fig. 30.1 and Table 30.1). This is why the OT hydrothermal systems are representative of the 'TAIGA of Methane.'

The chemical characteristics of venting hydrothermal fluid are primarily constrained by high-temperature fluid-rock interactions at deep hydrothermal reaction zones (Seewald and Seyfried 1990; Seyfried et al. 2003; German and von Damm 2003). Phase separation and subsequent phase segregation occurring at deep high-temperature region also affect the chemistry of the venting fluid (Gamo 1995). Furthermore, certain microbial and chemical effects on hydrothermal chemistry have been identified in the branched low-temperature diffusing fluid in the discharge stage (Butterfield et al. 2004; von Damm and Lilley 2004; Toki et al. 2008). These key processes, however, have been hypothesized to occur in the high-temperature hydrothermal reaction zones and during the discharge stage, not in the fluid recharge stage, where cool seawater penetrates into the subsurface and its chemistry changes with increasing temperature via relevant (bio)geochemical processes.

Recently, I and my colleagues have claimed that chemical and biological processes occurring in the recharge stage significantly affect the chemical composition of the venting fluid in the case that the product is inert under the conditions of the high-temperature hydrothermal reaction zone, such as methane (Kawagucci et al. 2011, 2013a). From this point of view, we have considered Microbial Methanogenesis at Recharge stage (MMR) in hydrothermal circulation as a possible predominant source of CH_4 in the high-temperature venting fluid, and refer to the concept as the 'MMR model' (Kawagucci et al. 2011). The MMR model is relevant particularly in a sediment-associated hydrothermal system, where the recharge stage of hydrothermal fluid circulation is expected to include an organic-rich sedimentary environment that promotes the widespread occurrence of functionally active microbial communities and impacts on fluid chemistry. Although the characteristic fluid chemistry in sediment-associated hydrothermal systems has occasionally been explained by equivocal 'fluid-sediment interaction', the MMR model argues that "fluid-sediment interaction" has been further classified into three types with respect to processes (microbial or chemical) and stages of subseafloor fluid circulation (recharge or discharge) (Kawagucci et al. 2013a).

In this chapter, I attempt to discover how and where the 'TAIGA of Methane' forms mainly based on fluid chemistry, following the recently proposed MMR model (Kawagucci et al. 2011, 2013a). For this purpose, general characteristics of the hydrothermal fluid chemistry of the OT fields are reviewed at first and then compared with those of other hydrothermal systems in Sect. 30.2. After assessing the utility of geochemical tracers to deduce the origin of hydrothermal fluid methane in Sect. 30.3, I discuss the geochemical origins of CH_4 dissolved in hydrothermal fluid in each OT field and their relevance with the geological setting and geographical distribution of hydrothermal fluid circulation in Sect. 30.4.

30.2 Major Fluid Chemistry

30.2.1 General View of the OT Hydrothermal Fluids

The OT hydrothermal fluids show significant enrichment of not only CH_4 but also of some other components (e.g., CO_2, K, NH_4, etc.) compared to hydrothermal fluids collected from sediment-starved Mid-Ocean Ridge (MOR) fields. Pioneering works (Sakai et al 1990a, 1990b; Gamo et al. 1991; You et al. 1994; Ishibashi et al. 1995) noted that the distinctive chemistry of the OT hydrothermal fluids is linked with the organic-rich continent-derived sediment filling the OT seafloor and the volatile-rich dacitic-rhyolitic (silicic) magma beneath the OT. Moreover, relatively shallow water depths of the OT hydrothermal systems (Fig. 30.1) serve as a physical factor that induces frequent boiling (subcritical phase separation) and subsequent phase segregation (Fig. 30.2), which results in chemical compositions of the venting hydrothermal fluids that are quite different from the deep source fluid (Gamo 1995). Phase separation forces volatile species into the resulting 'vapor' phase and leaves ion species in the 'liquid' phase. The source hydrothermal fluid composition prior to the phase separation can be estimated by a simple correction using the venting fluid chlorine concentration (i.e., the ion-element/Cl ratio) (Butterfield et al. 2003). Despite potential influences of multiple factors due to the geological and tectonic backgrounds of the OT, limited observations at each sediment-associated basalt-hosted MOR system and sediment-starved silicic rock-hosted arc-back-arc (ABA) system in the early 1990s inhibited the understanding of how the sediment filling the OT seafloor and volatile-rich silicic host rocks impact the OT hydrothermal fluid chemistry. Over the 35 years since the discovery of deep-sea hydrothermal activity in 1977, the current global dataset of hydrothermal fluid chemistry has enabled us to compare the fluid chemistry of the OT fields with that of hydrothermal systems of various geological and tectonic backgrounds. Field-to-field variations (inter-field variation) of fluid

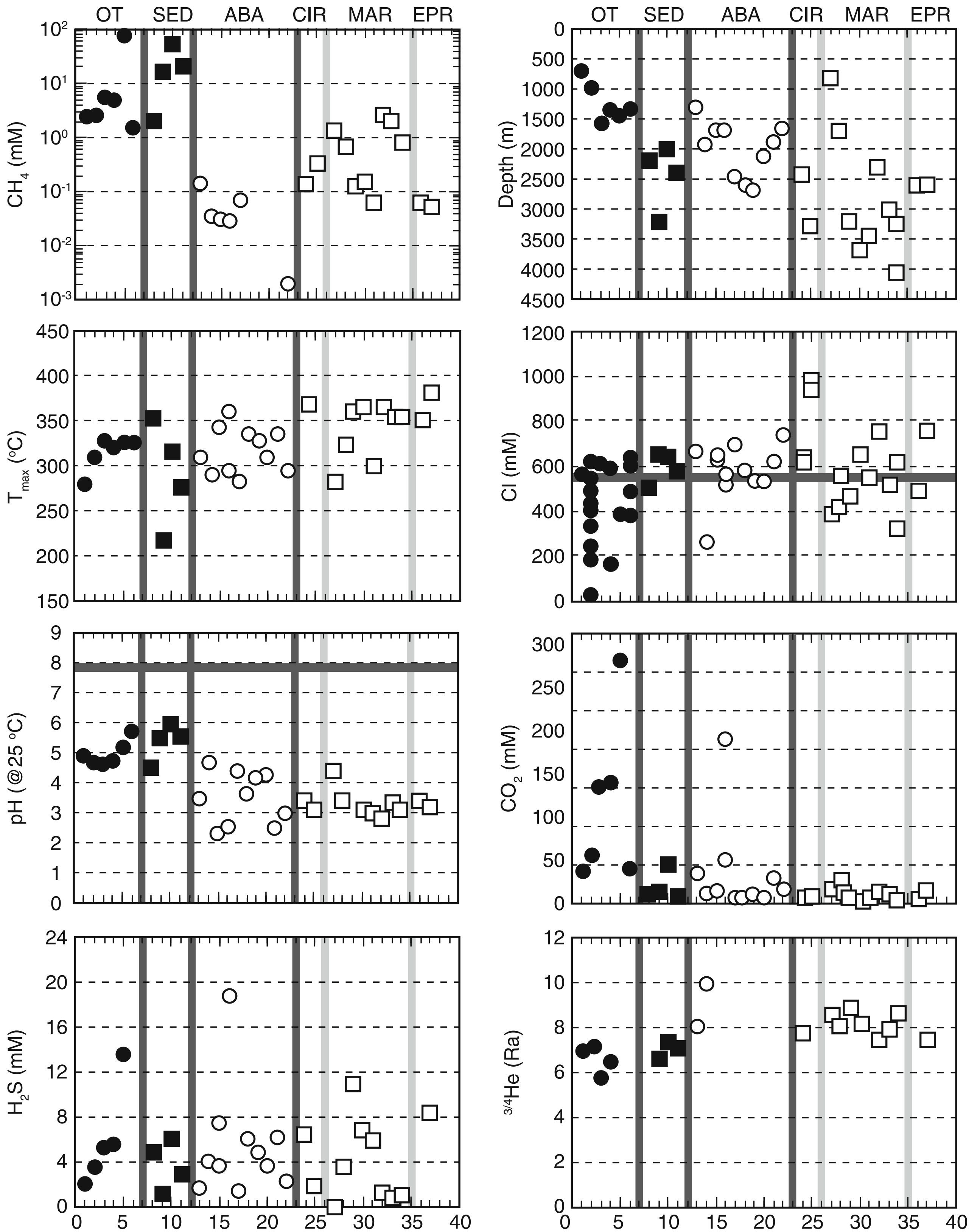

Fig. 30.1 Compilation of the physical properties and fluid chemistry of the Okinawa Trough and global hydrothermal fields. The vertical axis (methane concentration) is in logarithm scale. Horizontal axes are common for all panels and represent each hydrothermal field as follows: 1-Minami-Ensei, 2-Iheya North, 3-Hakurei, 4-Jade, 5-Hatoma, 6-Daiyon-Yonaguni, 7-vacant, 8-Endeavour, 9-Escanaba, 10-Guaymas, 11-Middle Valley, 12-vacant, 13-Suiyo, 14-North Fiji, 15-Roman Ruins, 16-Satanic Mills, 17-Vienna Woods, 18-Kilo Moana, 19-Tow Cam, 20-ABE, 21-Mariner, 22-Brother, 23-vacant, 24-Kairei, 25-Edmond, 26-vacanct, 27-Manez Gwen, 28-Lucky Strike, 29-Broken Spur, 30-TAG, 31-Snake Pit, 32-Rainbow, 33-Logatchev, 34-Ashadze, 35-vacant, 36-EPR21N, 37-EPR13N. *Vertical dark* and *light gray bars* separate different geological/tectonic settings. *Horizontal gray bars* in several panels represent seawater levels. References for this figure are presented in Sect. 30.2.2

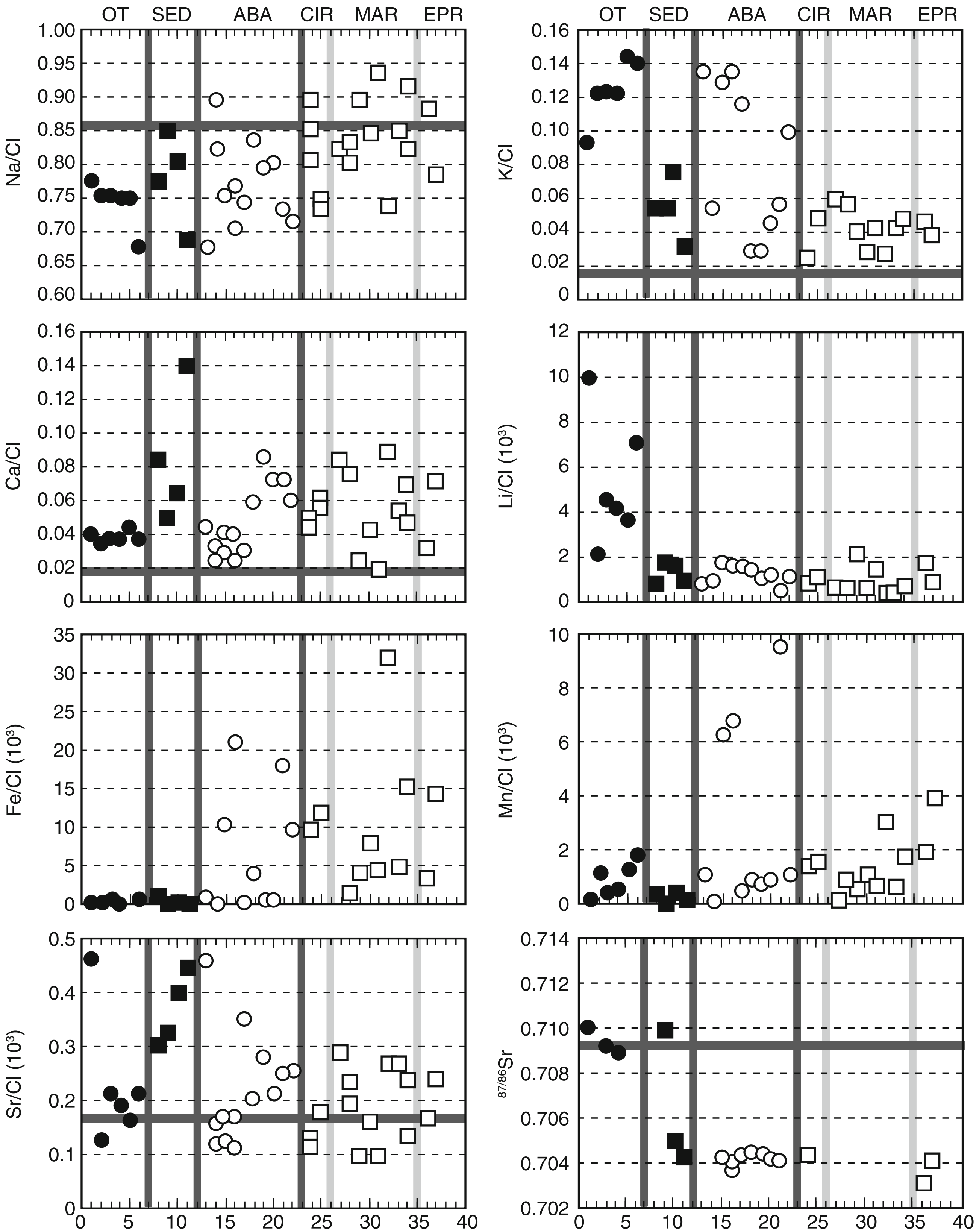

Fig. 30.1 (continued)

Table 30.1 Fluid chemistry of the Okinawa Trough hydrothermal fields

		Iheya North		Izena Hall			Hatoma	Daiyon-Yonaguni		
Field vent	Minami Ensei (whole)	NBC 2011	Variation	Jade	Hakurei	Biwako	Gusuku	Lion	Variation	Seawater
Depth (m)	700	980		1,350	1,600	1,525	1,473	1,360		
T_{max} (°C)	280	309	<311	320	326	104	325	325	<328	
pH	4.9	4.65	>4.65	4.7	4.7	4.8	5.2	5.7	5.7–6.8	7.8
Alk. (mM)	3.3	1.3	0.2–3.3	1.5	1.5		4.7	0.25	0.25–2.95	2.3
Cl (mM)	562	599	16–634	590	608	167	381	614	376–635	559
Na (mM)	436	451	8–479	442	458	173	285	416	254–433	480
K (mM)	53	73	7–82	72	75	12	55	86	55.3–90.1	10
Ca (mM)	23	21.1	0–25	22	23	4.3	17	23.2	14.3–26.1	11
Si (mM)	11.1	11.9	3.1–13.8	11.8	11.3	11	12	11.3	11.3–13.2	0.18
B (mM)	3.8	1.97	0.44–2.3	3.2	3.7	1	3.3	3.9	2.93–4.31	0.43
Li (mM)	5.6	1.32	0.11–1.52	2.5	2.8		1.4	4.4		0.026
Fe (μM)	120	121	31–142	31	445		8.6	410	80–410	0.001
Mn (μM)	99	694	115–694	341	290		483	1,120	700–1,250	0.003
Ba (μM)		31	9.7–44	65	120					0.15
Al (μM)	4.7	11.0								0.04
Sr (μM)	260	77		115	129	27	62	130		91
$^{87/86}Sr$	0.71			0.7089	(0.7094)					0.70918
F (μM)		209								70
Br (μM)		952								860
I (μM)	30	44.8								0.5
Mo (nM)							7			107
W (nM)		320					123			0.07
Zn (μM)		94								0.01
Se (nM)		73		40–150	50–100					2.3
CH_4 (mM)	2.4	2.5	0.2–7.0	4.9	6.8		80	1.6	1.2–13.5	0.0000001
$\delta^{13}C_{CH4}$ (‰)	−25	−54.1	−58.2 to −54.0	−30.8	−32.1		−50	−26.9	−27.3 to −24.8	
δD_{CH4} (‰)	−112	−124	−132 to −113	−113	−113					
H_2 (mM)	0.04	0.10	0.03–0.2	0.06	1.4		0.2	1.0	0.8–5.5	0.0000001
δD_{H2} (‰)	−420	−394	−430 to −394	−381	−379		−386			
CO_2 (mM)	42	63	27–228	156	151		315	47	22–329	2.3
$\delta^{13}C_{CO2}$ (‰)	−5.1	−9.6	−10.8 to −8.8	−6.2	−6.2		−7.9	−7.3	−8.0 to −7.2	−8
δD_{H2O} (‰)		−1.0		−0.3	−0.6					0
$\delta^{18}O_{H2O}$ (‰)		+1.2		+1.8	+1.6					0
NH_4^+ (mM)	5.4	2.1	1.6–3.9	4.2	4.4	5	7.2	14.7	8.6–14.7	
H_2S (mM)	2	3.6	1.8–3.9	5.6	5.2	23	13.5			0.0000001
$\delta^{34}S_{H2S}$	+3.6	+11		+3.6 to +7.7	+5.5 to +7.8					
C_2H_6 (uM)	<1	<1		0.33	2.5					
CO (uM)				30	63					0.0001
He (uM)	0.68			0.72	0.53					
$^{3/4}He$ (R_{atm})	6.99	7.1		6.5	5.81					1

chemistry among the global hydrothermal fields help to clarify the characteristic fluid chemistries of the OT hydrothermal fluids and their relationships with geological and tectonic backgrounds.

This chapter discusses only the 'endmember' high-temperature fluid chemistry, estimated by a Mg-diagram and extrapolation of Mg concentrations to zero (von Damm et al. 1985), to avoid losing focus on the inter-field comparison. Thus this chapter does not discuss secondary chemical modification associated with either low-temperature hydrothermal fluid discharges through the sedimentary environment (Gamo et al. 1991; Kawagucci et al. 2013b; Yokoyama et al. Chap. 31) or the liquid CO_2 emersion and the relevant microbial ecosystems (Inagaki et al. 2006; Yanagawa et al.

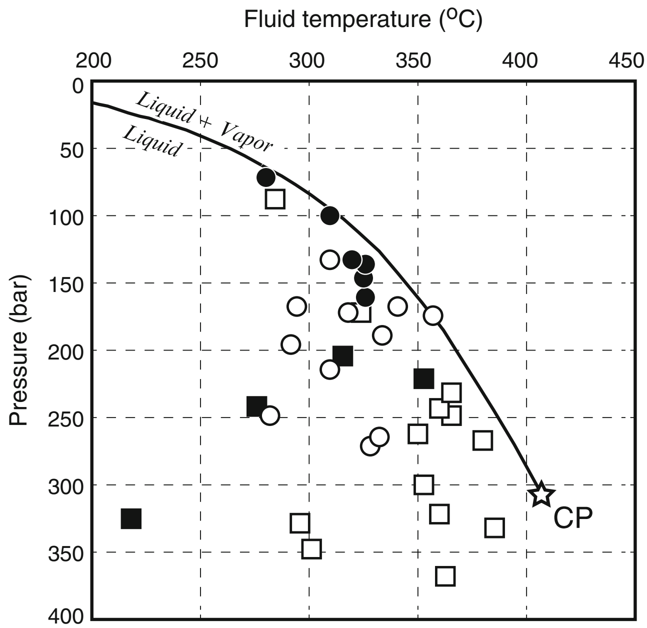

Fig. 30.2 Two-phase curve for seawater. Each symbol represents P-T conditions of venting fluids at each field from the Okinawa Trough (*filled circles*), sediment-associated systems (*filled squares*), sediment-starved ABA systems (*open circles*), and sediment-starved MOR systems (*open squares*). An open star (CP) represents a critical point of seawater. References for this figure are presented in Sect. 30.2.2

2013). In addition, trace elements (Mo, W, REE, etc.) measured in some OT hydrothermal fluids (Kishida et al. 2004; Hongo et al. 2007; Kawagucci et al. 2013b) are also not included in this chapter because the limited available dataset prohibits global comparison.

30.2.2 Inter-Field (Field-to-Field) Variation and the OT Characteristics

Figure 30.1 shows the physical properties and the Mg-corrected endmember chemistries of high-temperature hydrothermal fluids in (1) the six OT fields (Table 30.1), (2) four sediment-associated MOR fields (Lilley et al. 1993, 2003; Proskurowski et al. 2004, 2006; von Damm et al. 2005; McCollom 2008; Ishibashi et al. 2002; Pearson et al. 2005; Gieskes et al. 2002; Butterfield et al. 1994; and references therein), (3) ten sediment-starved ABA fields (Tsunogai et al. 1994, 2005; Toki et al. 2008; Kishida et al. 2004; Ishibashi et al. 1994a, 1994b; 2002b; Grimaud et al. 1991; Reeves et al. 2011; Mottl et al. 2011; de Ronde et al. 2011; and references therein), and (4) twelve sediment-starved MOR fields (Gamo et al. 2001; Kumagai et al. 2008; Gallant and von Damm 2006; Fouquet et al. 2010; Charlou et al. 2010; Von Damm et al. 1985; Merlivat et al. 1987; and references therein). The hydrothermal fields shown in Fig. 30.1 represent global variations in host rock chemistry (silicic, mafic, and ultramafic) and geographical distribution (the Indian Ocean, the Pacific Ocean, the Atlantic Ocean, and the adjacent seas). The endmember Cl concentrations are deviated from seawater Cl levels in almost all the hydrothermal fields (Fig. 30.1), demonstrating alteration in fluid chemistry due to the phase separation. For ion species, element/Cl ratios are used instead of concentrations to eliminate the effect of phase separation (Fig. 30.1).

The highest measured temperatures of hydrothermal fluids (T_{max}) in the OT hydrothermal fields range between 280 and 326 °C, which are lower than typical T_{max} of the MOR fields (approximately 350 °C). Fluid temperature is very likely constrained by pressure, which determines the fluid boiling temperature (Fig. 30.2). Because the water depths of the OT hydrothermal fields range between 700 and 1,600 m and are generally shallower than other hydrothermal systems (Fig. 30.1), the pressure condition (the potential of T_{max}) is lower. In fact, the fluid pressure-temperature conditions of the OT fields are very close to the two-phase boundary (Bischoff and Rosenbauer 1984) (Fig. 30.2).

The hydrothermal fluid pH of the OT fields, measured at 25 °C in an onboard laboratory, range from 4.65 to 5.7. This pH range is generally comparable with that in the sediment-associated MOR systems (pH = 4.5–5.9) but higher than the pH ranges of sediment-starved ABA and MOR systems (pH = 2–5) (Fig. 30.1). In addition, a low-temperature hydrothermal fluid with an extremely low pH (≤2.1) due to direct emission of magmatic SO_2 to the seafloor has been observed in the DESMOS field in the eastern Manus Basin, Western Pacific (Gamo et al. 1997). The moderately acidic pH of the OT fluids despite the ABA tectonic background suggests that some components from sedimentary organic matter decomposition, such as millimolar levels of NH_3/NH_4^+ (Table 30.1), buffer the pH. The presence of NH_3/NH_4^+ in high-temperature hydrothermal fluids is known to yield a high pH at the 25 °C measurement but a lower pH at in situ hydrothermal conditions (Tivey et al. 1999). The OT hydrothermal fluids contain abundant CO_2 (>40 mM) of magmatic origin, based on the carbon isotope ratios of the CO_2 (Ishibashi et al. 1995; Kawagucci et al. 2011, 2013a). In contrast, the concentrations of H_2S, another major component of the magma-derived volatiles, are similar between the OT and other fields, regardless of the geological/tectonic backgrounds (Fig. 30.1). The helium isotope ratios ($^{3/4}$He) of the OT hydrothermal fluids are ≤7.1 and are similar to those in the sediment-associated MOR fluids (Fig. 30.1). This $^{3/4}$He range, which is slightly lower than the typical sediment-starved MOR value of 8 (Sano and Fischer 2013), implies a contribution of crustal ^{4}He-enriched helium.

The lower Na/Cl ratios of the OT fluids (0.68–0.78) compared to the seawater Na/Cl ratio (0.86) suggest Na uptake into the solid phase during subseafloor fluid circulation (Fig. 30.1). High K/Cl ratios are typical characteristics of hydrothermal fields in ABA systems, including the OT fields (>0.09) (Fig. 30.1). The K enrichment in the ABA fluids is attributed to probable K enrichment in surrounding rocks, with which fluid interacts during fluid circulation (Sakai et al. 1990a). The magnitudes of Na-loss and K-gain in each OT field seem consistent between each other (Fig. 30.1), implying quantitative exchange of Na for K during fluid-mineral interaction. In addition, a geographical trend in the K/Cl variation within the OT is also found: higher K/Cl ratios in southern OT fields (Daiyon-Yonaguni and Hatoma) than in northern OT fields (particularly Minami-Ensei). This trend may reflect a difference in the K content of the basement rocks, although there is little data on the host rock chemistry of the OT hydrothermal fields (Shinjo and Kato 2000). The Ca/Cl ratios are lower in the OT fields (<0.05) than in the others, including sediment-associated MOR fields (Fig. 30.1). The Li/Cl ratios are substantially higher in all of the OT fields (>0.002) than in the other fields. Because of the almost quantitative partitioning of alkali elements into the fluid phase during high-temperature fluid-rock (-sediment) interactions, the high Li/Cl ratios in the OT fluids suggest Li enrichment in the OT basement rocks and/or the OT-filling sediment. Low Fe/Cl ratios (<0.001) are typical in the sediment-associated fields while the low Fe/Cl ratios of the OT fluids may be associated with low T_{max}. The Mn/Cl ratios are similar regardless of tectonic/geological background, excluding several ABA fields where the Mn/Cl ratios are extremely high. The Sr/Cl ratios so far observed in hydrothermal fluids vary among the fields regardless of tectonic/geological backgrounds. The hydrothermal fluid Sr/Cl range, higher or lower than the seawater Sr/Cl ratio in each field, indicates that both net gain and loss of Sr from the starting seawater during the hydrothermal fluid circulation is possible. Strontium isotope ratios ($^{87/86}$Sr) are high (≥0.709) in the OT Minami-Ensei and Jade fields (Noguchi et al. 2011) and a sediment-covered Escanaba field but low (approximately 0.704) in sediment-starved MOR and ABA fields and sediment-covered Guaymas and Middle Valley fields. The high $^{87/86}$Sr ratios of the OT fluids are attributed to those in the OT-filling sedimentary component (Noguchi et al. 2011).

30.3 Gas Species Chemistry

30.3.1 Methane Sources in Hydrothermal System

The chemical origins of subseafloor CH_4 are typically classified by a combination of the carbon source (inorganic or organic) and the generation process (chemical or biological,

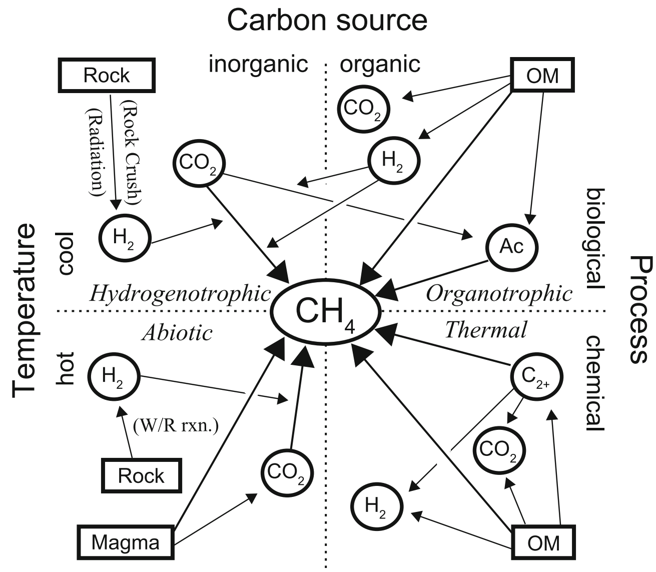

Fig. 30.3 Schematic illustrating methanogenic pathways in subseafloor geofluid systems. Ac, C_{2+}, and OM represent acetate, hydrocarbons with carbon numbers >2, and organic matter, respectively. After Kawagucci et al. (2013a) with minor modification

which approximately correspond to high-temperature or low-temperature environments) (Fig. 30.3). This classification distinguishes three types: so-called abiotic CH_4 (e.g., McCollom 2013), thermogenic CH_4 (e.g., Welhan and Lupton 1987), and biogenic CH_4 (e.g., Valentine et al. 2004). Abiotic CH_4 has been considered to be the predominant source of hydrothermal fluid CH_4 in typical sediment-starved hydrothermal systems. However, in almost all the sediment-starved hydrothermal fields so far observed, the measured CH_4 concentrations are several orders of magnitude greater (or smaller) than the CH_4 concentrations that are thermodynamically predicted from the H_2 and CO_2 concentrations and fluid temperature of the venting fluid (McCollom 2008). While the excess could be explained by the loss of H_2 and/or CO_2 during fluid upwelling from the deep zone where abiotic methanogenesis has actually occurred, CH_4 derived from other sources could also account for the excess. Thermogenic CH_4 has been thought to be the predominant source for abundant CH_4 in hydrothermal systems occurring close to sedimentary organic-rich environments, such as the OT fields (Ishibashi et al. 1995). Even if the seafloor has a sediment-starved appearance, organic matter buried beneath the seafloor is assumed to be a source for thermogenic CH_4 (Lilley et al. 1993). Biogenic CH_4 includes methane generated by both hydrogenotrophic and organotrophic methanogenesis. The microbial syntrophic relationship between fermentative hydrogenogenesis and hydrogenotrophic methanogenesis is expected in the sedimentary environment (Fig. 30.3). Biogenic CH_4 could be incorporated into hydrothermal fluid only in the recharge stage of the whole fluid circulation process because the reaction zone and the discharge stage are too hot for any microbes to be active (Takai et al. 2008). The recharge stage environment, where the penetrating seawater becomes reduced and warm, is very likely suitable for anaerobic and/or thermophilic microbes.

The MMR model, which we have proposed in recent papers (Kawagucci et al. 2011, 2013a), describes the origin of hydrothermal fluid CH_4 in not only geochemical terms but also geographical aspects. This model claims that CH_4 in high-temperature hydrothermal fluid can originate from CH_4 that is generated biologically and incorporated into the fluid in the low-temperature recharge stage of hydrothermal fluid circulation. The MMR model is emphasized particularly in the sediment-associated hydrothermal systems where the recharge stage of hydrothermal fluid circulation is expected to include an organic-rich sedimentary environment. Even if the sedimentary recharge zone is absent, methanogenic ecosystems in the crustal recharge zone might be fueled by abiotic H_2 generated from serpentinization (McCollom and Bach 2009), water radiolysis (Lin et al. 2005), and/or fault activity (Hirose et al. 2011). Moreover, abiotic methanogenesis associated with serpentinization of ultramafic rocks in the recharge stage cannot be ruled out because of its kinetic and thermodynamic favorability at temperatures of 200–315 °C (McCollom and Bach 2009). Consequently, all three types of CH_4 generation and their occurrence through each stage of the whole fluid circulation system should be considered to deduce the origins of CH_4 in venting hydrothermal fluid.

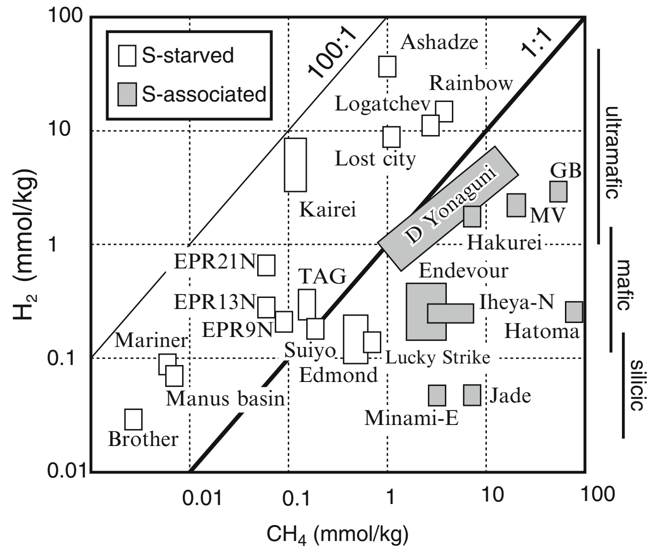

Fig. 30.4 Plots of H_2 concentration versus CH_4 concentration in hydrothermal fluids. *Open* and *gray squares* represent sediment-starved and sediment-associated fields, respectively. *Vertical bars* indicate typical H_2 concentrations in reaction zone fluids for silicic, mafic, and ultra-mafic basement systems. Labels GB and MV are Guaymas Basin and Middle Valley, respectively. After Kawagucci et al. (2013a) with minor modification

30.3.2 Geochemical Tracers to Deduce the Origin of Methane

The origin of hydrothermal fluid CH_4 can be deduced by using geochemical tracers, and the multiple tracers approach allows us to more accurately deduce the origin of hydrothermal fluid CH_4. Although several tracers have been proposed and indeed utilized, the indications of the tracers include uncertainties in some circumstances and should be assessed carefully. This issue has already been discussed in previous papers on stable hydrogen isotope ratios (δD_{CH4}) (Kawagucci et al. 2011), stable carbon isotope ratios ($\delta^{13}C_{CH4}$), relative abundances of CH_4 to non-methane hydrocarbons (C_1/C_{2+}), and H_2 concentrations (Kawagucci et al. 2013a). Here, a summary of the previous discussion with some additional information is presented.

30.3.2.1 Methane Concentration and $CH_4/^3He$ Ratio

The concentration of CH_4 in the venting fluid is a fundamental piece of information in deducing the origin of the CH_4. The global dataset of high-temperature hydrothermal fluid compositions illustrates two approximate relationships between CH_4 concentrations and geological settings. First, CH_4 concentrations are significantly higher in hydrothermal fields located in sedimentary locations (Figs. 30.1 and 30.3). This type of CH_4 enrichment typically accompanies enrichment in certain other components, such as ammonium, suggesting anoxic organic matter decomposition for its origin. Second, CH_4 concentrations are approximately related to the redox state of the rocks exposed around the vents: higher CH_4 concentrations are associated with more reduced rocks (Figs. 30.1 and 30.4). Although, again, measured CH_4 concentrations are not consistent with thermodynamic predictions (McCollom 2008), more reducing conditions in the reaction zone are advantageous for abiotic methanogenesis.

The relative abundance of CH_4 with ^3He ($CH_4/^3He$) differentiates mantle-derived CH_4 from crust- and sediment-derived CH_4 because juvenile ^3He should be derived from the mantle. $CH_4/^3He$ ratios higher than 10^7 (mol/mol) are typically found in sediment-associated hydrothermal fields (Lilley et al. 1993; Ishibashi et al. 1995) and sediment-starved slow-spreading MOR fields (Charlou et al. 2000), while ratios of 10^6 are reported for moderate- to fast-spreading MOR hydrothermal fields (Kawagucci et al. 2008; and references therein).

30.3.2.2 Carbon and Hydrogen Isotope Ratios of Methane

The $\delta^{13}C_{CH4}$ value is the geochemical indicator most widely used to deduce the origins of environmental CH_4. Expected ranges of $\delta^{13}C_{CH4}$ values for each of the three types have been investigated in laboratory experiments (Fig. 30.5). The $\delta^{13}C_{CH4}$ values of abiotic CH_4 in the experiments (−40 to −20 ‰) (e.g., Horita and Berndt 1999; McCollom and Seewald 2006; McCollom et al. 2010) are quite different from those frequently observed in the sediment-starved hydrothermal fields (−20 to −5 ‰). The inconsistency in abiotic $\delta^{13}C_{CH4}$ values remains unresolved. I suspect the reason may be due to some experimental artifacts, such as unnatural catalysts of Fe-Ni alloy, for example. Thermogenic CH_4 generated from sedimentary organic matter ($\delta^{13}C_{org}$ = −25 to −20 ‰) likely results in $\delta^{13}C_{CH4}$ values between −30 and −20 ‰ because of small isotope fractionation, based on experiments (Seewald et al. 1994). However, larger fractionations at lower temperature (Hoefs 2009) and intra-molecular ^{13}C depletion in the methyl-carbon of long-chain hydrocarbons (Gilbert et al. 2013) imply possibly more ^{13}C-depleted thermogenic CH_4. Although a broad $\delta^{13}C_{CH4}$ range (−50 to −20 ‰) was proposed for thermogenic CH_4 based on the compilation of field observations (Whiticar 1999), such a broad range may result from the mixing of 'pure' thermogenic CH_4 described above with ^{13}C-depleted biogenic CH_4 (−100 to −40 ‰) (Kawagucci et al. 2013a and references therein). The $\delta^{13}C_{CH4}$ values at the time of generation might be modified by certain processes occurring during subseafloor fluid migration (e.g., carbon isotope exchange between CO_2-CH_4), but the $\delta^{13}C_{CH4}$ modifications are expected to be negligible in terms of both reaction kinetics and/or magnitudes of the fractionation (see Kawagucci et al. 2013a for details). Consequently, the $\delta^{13}C_{CH4}$ value is a robust and useful indicator for deducing the origin of subseafloor CH_4.

The δD_{CH4} value has been used as an indicator to deduce the origin of environmental CH_4, in addition to the $\delta^{13}C_{CH4}$ value (Fig. 30.6). Many incubation experiments using both microbial isolates and bulk ecosystems (e.g., soil) revealed that biogenic CH_4 displayed a typically D-depleted isotope signature (−350 to −250 ‰) (Sugimoto and Wada 1995; Valentine et al. 2004) at the case that the δD_{H2O} value is +0 ‰. These incubations also revealed that the empirical $\delta D_{CH4}/\delta D_{H2O}$ ratio is approximately 0.75 for hydrogenotrophic methanogenesis and approximately 0.25 for aceticlastic methanogenesis. In contrast, past compilations of observations from sediment, oil fields, and natural gases (Nakai et al. 1974; Whiticar 1999) proposed a broader range of δD_{CH4} values (−450 to −150 ‰) as the "biogenic methane signature." The proposed biogenic δD_{CH4} characteristics from the compilation should be followed with care because environmental CH_4 may result

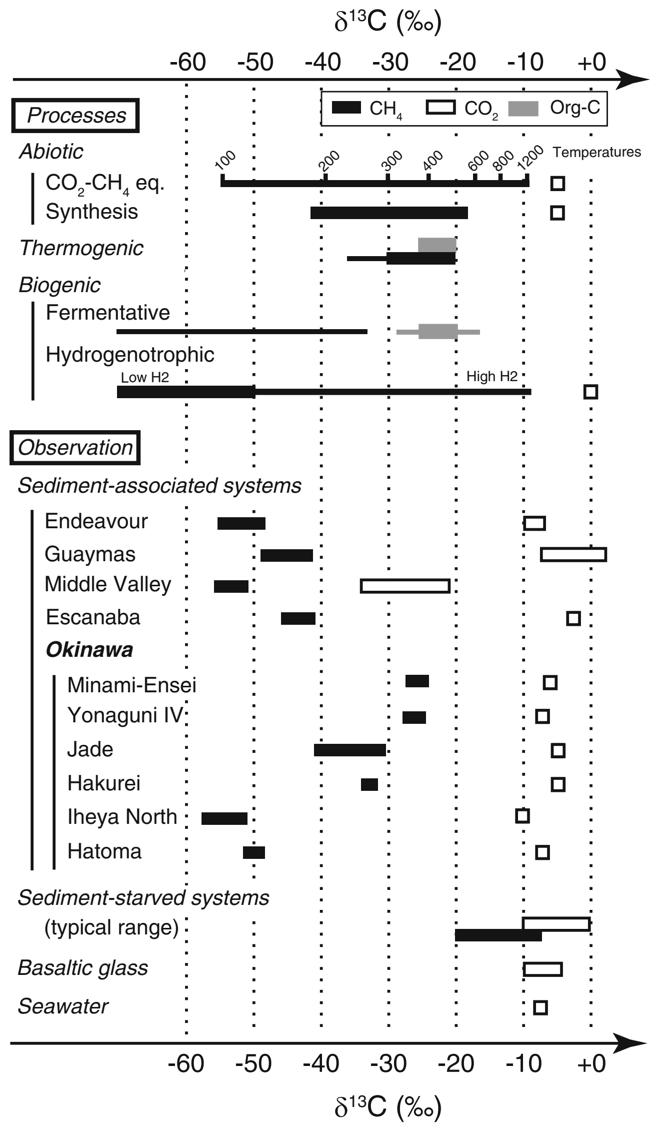

Fig. 30.5 $\delta^{13}C$ values of CH_4 (*black bars*), CO_2 (*white boxes*), and organic carbon (*gray bars*) considered typical for each process based on experimental and theoretical studies and observations in hydrothermal fluids. After Kawagucci et al. (2013a) with minor modification

from the mixing of multiple CH_4 sources and may have been partly consumed that results in increase of δD_{CH4} value. Nevertheless, all hydrothermal δD_{CH4} values measured so far have fallen into a narrow range (−130 to −96 ‰), regardless of the types of hydrothermal systems (Proskurowski et al. 2006; Kawagucci et al. 2011, 2013a; Reeves et al. 2011). This narrow range is very likely caused by hydrogen isotopic equilibrium between CH_4 and H_2O in the high-temperature fluids (>250 °C and δD_{H2O} = +0 ‰) that lead to δD_{CH4} values of approximately −130 ‰ (Proskurowski et al. 2006) although the certain reaction kinetics of hydrogen isotope exchange between CH_4 and H_2O toward isotopic equilibrium have never been

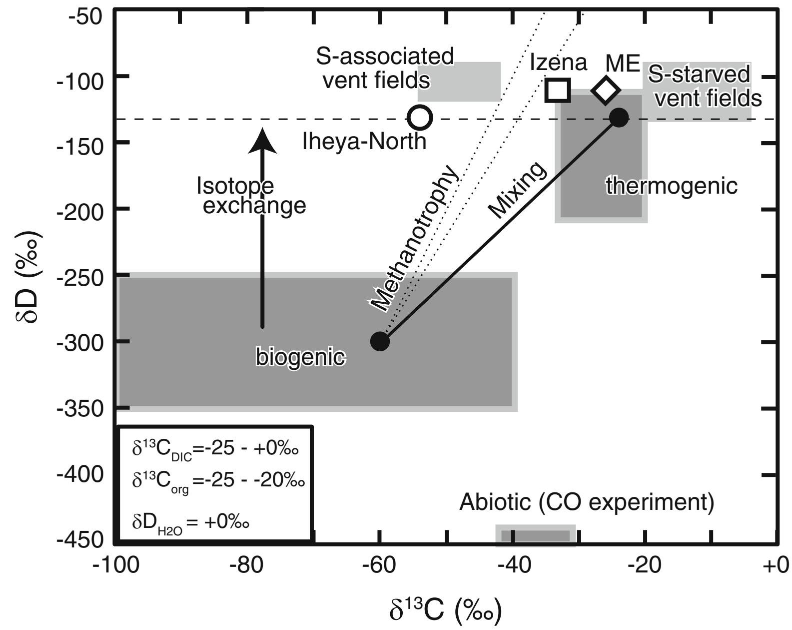

Fig. 30.6 Plots of δD_{CH4} values versus $\delta^{13}C_{CH4}$ values. *Open symbols* represent the observations in the Okinawa Trough (ME: Minami-Ensei; Izena: Jade and Hakurei). *Light gray areas* represent typical ranges of sediment-starved and -associated fields as labeled. *Dark gray areas* represent the expected ranges for thermogenic, biogenic, and abiotic methane, where the values of $\delta^{13}C_{DIC}$ (−25 to +0 ‰), $\delta^{13}C_{org}$ (−25 to −20 ‰), and δD_{H2O} (+0 ‰) are assumed for a methanogenic environment (see literature for details). An *arrow* and a *horizontal break line* represent the direction of δD_{CH4} change on the hydrogen isotope exchange between H_2O and CH_4 and the value at the isotope equilibrium, respectively. *Diagonal dotted lines* represent typical co-variation of $\delta^{13}C$-δD in microbial methane consumption ($\Delta\delta D/\Delta\delta^{13}C = 8$–10) (Feisthauer et al. 2011)

constrained (Reeves et al. 2012). While no experiment has yet verified the δD_{CH4} value of thermogenic CH_4, the δD_{CH4} values would be dominated by subsequent isotope exchange resulting in the isotopic equilibrium due to the obligatory high temperature. In addition, experimentally estimated δD_{CH4} values for abiotic CH_4 (e.g., approximately −500 ‰) (McCollom et al. 2010) (Fig. 30.6) are quite different from the isotopically equilibrated δD_{CH4} values, despite high-temperature condition for the methanogenesis. The presence of both equilibrated δD_{CH4} values and non-equilibrated $\delta^{13}C_{CH4}$ values in a CH_4 reservoir would be reasonable because the molecular geometry of CH_4 (carbon as a central atom and hydrogen as terminal atoms) suggests more rapid exchange of hydrogen. Consequently, the δD_{CH4} value is, in general, not useful in deducing the origin of hydrothermal fluid CH_4 due to the predominance of secondary isotope exchange. However, co-variation of $\delta^{13}C$ and δD ($\Delta\delta D/\Delta\delta^{13}C = 8$–10) has been identified in microbial methanotrophic activity (Feisthauer et al. 2011). Therefore, combination measurements between δD_{CH4} and $\delta^{13}C_{CH4}$ for a series of fluid samples provides supporting information for discussion of whether the $\delta^{13}C_{CH4}$ values of the samples have been altered by microbial methanotrophy (Fig. 30.6).

The radioactive carbon in CH_4 ($\Delta^{14}C_{CH4}$) is a possible tracer. Because magma-derived carbon should be ^{14}C-dead, detectable ^{14}C in hydrothermal fluid CH_4 indicates carbon input from seawater or young sediment. Therefore, detectable ^{14}C in the hydrothermal fluid CH_4, if present, implies microbial methanogenesis in the recharge stage of hydrothermal fluid circulation as a dominant CH_4 source. As far as the author is aware, only one study, which used samples from the sediment-covered Guaymas hydrothermal field, has reported ^{14}C measurements of high-temperature hydrothermal fluid CH_4 (Pearson et al. 2005) that revealed ^{14}C-dead CH_4 in hydrothermal fluid.

30.3.2.3 Molecular Hydrogen and Non-methane Hydrocarbons

The concentration of H_2 in hydrothermal fluid primarily depends on the redox conditions of the high-temperature hydrothermal reaction zone. In fact, a clear relationship between the host rock type (ultramafic to silicic) and the measured H_2 concentration has been identified in sediment-starved fields (Fig. 30.4). The relationship is also found even in several sediment-associated fields, such as the OT Minami-Ensei and Jade fields (Fig. 30.4). Because H_2 is likely buffered in the reaction zone by rapid reaction kinetics, additions of H_2 in the recharge stage of hydrothermal fluid circulation would be diminished in the reaction zone and never detectable in the venting fluid. In turn, because sub-millimolar levels of H_2 are expected from mafic host rocks, the measured millimolar levels of H_2 in hydrothermal fluids in the fully sediment-covered mafic-hosted Guaymas and Middle Valley fields are attributed to thermogenic H_2 input during the discharge stage of hydrothermal fluid circulation. Consequently, the H_2 concentration of the venting fluid is a useful indicator in determining whether thermal fluid-sediment interaction occurred in the discharge stage.

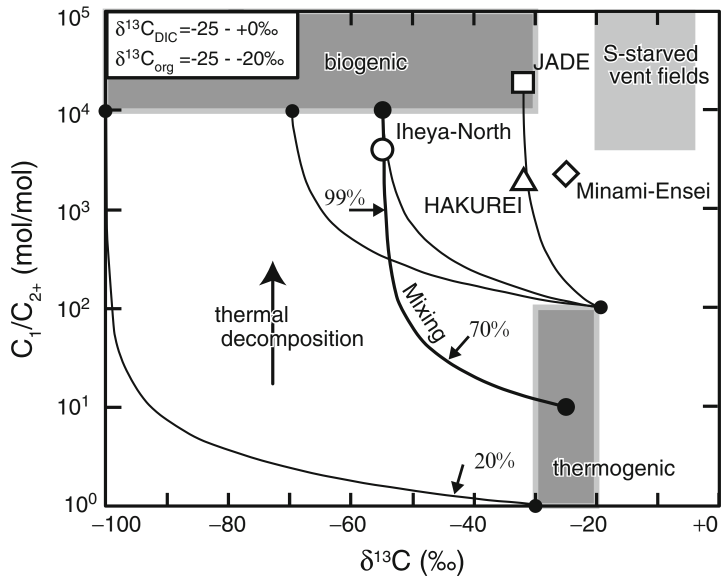

Fig. 30.7 A diagram of C_1/C_{2+} ratios versus $\delta^{13}C_{CH4}$ values. *Gray areas* represent the expected ranges of each hydrocarbon source, estimated by assuming $\delta^{13}C_{DIC}$ (−25 ‰ to +0 ‰) and $\delta^{13}C_{org}$ (−25 to −20 ‰) (see Kawagucci et al. (2013a)). Abiotic methane range is not described. Five curves demonstrate bimodal mixing scenarios between biogenic and thermogenic hydrocarbons. The *bold curve* is considered the most likely scenario for subseafloor environments in sediment-associated hydrothermal systems at this time. *Arrows* with percentages present contributions of biogenic methane at the arrowed points of the bimodal mixing curves. *Open symbols* represent the measured values in each Okinawa Trough hydrothermal field. After Kawagucci et al. (2013a) with minor modification

The C_1/C_{2+} ratio has been often utilized to deduce the origins of subseafloor CH_4 (Fig. 30.7). Although hydrothermal experiments demonstrating abiotic CH_4 generation have shown broad ranges of C_1/C_{2+} ratios of $>10^3$ (Horita and Berndt 1999) and approximately 3 (McCollom and Seewald 2006; McCollom et al. 2010), the observed range in sediment-starved hydrothermal fields is typically $>10^3$ (McCollom 2008 and references therein). The difference may be due to experimental artifacts, such as the use of unnatural catalysts of native iron, for example. Microbial methanogenesis accompanies little C_{2+} hydrocarbon generation and is expected to feature C_1/C_{2+} ratios of $>10^4$ (Kawagucci et al. 2013a; and references therein). While the C_1/C_{2+} ratios of thermogenic hydrocarbons under high-temperature hydrothermal conditions have not yet been experimentally verified, a C_1/C_{2+} ratio of $<10^2$ has been practically used as a thermogenic hydrocarbon signature (e.g., Whiticar 1999). It should be noted that thermal decomposition of C_{2+} hydrocarbons to CH_4 would likely occur under deep-sea hydrothermal conditions due to both thermodynamic and kinetic aspects and could result in increasing C_1/C_{2+} ratios as high as those of abiotic/biogenic CH_4 (Kawagucci et al. 2013a). It should also be noted that a C_1/C_{2+} ratio resulting from bimodal mixing between typical thermogenic hydrocarbons and biogenic CH_4 is not linearly correlated with the mixing ratio of CH_4 between these hydrocarbons (Fig. 30.7). Consequently, low C_1/C_{2+} ratios ($<10^3$) are a definite indication of thermogenic hydrocarbons contributions to the fluid, whereas higher C_1/C_{2+} ratios ($>10^3$) do not rule out involvement of thermogenic hydrocarbons.

30.4 Estimation of Fluid Circulation Path: Implications of Methane Geochemistry

By using the multiple tracers discussed above, the geochemical origins of the hydrothermal fluid CH_4 in each OT field and the relationships with the geological settings can be modeled in two-dimension schematic illustrations (Fig. 30.8). This modeling enables us to deduce the geographical distribution of hydrothermal fluid circulation (Kawagucci et al. 2013a). I attempt to discover the geographical distribution of fluid circulations for all six OT hydrothermal fields, with the addition of the OT bathymetry. It should be noted that almost all of the hydrothermal fluid vents of the OT fields are hosted in volcanic bodies that outcrop from the sediment that fills the OT.

30.4.1 Iheya North

The Iheya North hydrothermal fluid features low $\delta^{13}C_{CH4}$ values (−58 to −51 ‰), high C_1/C_{2+} ratios (>3,700), equilibrated δD_{CH4} values (−130 ‰), and low H_2

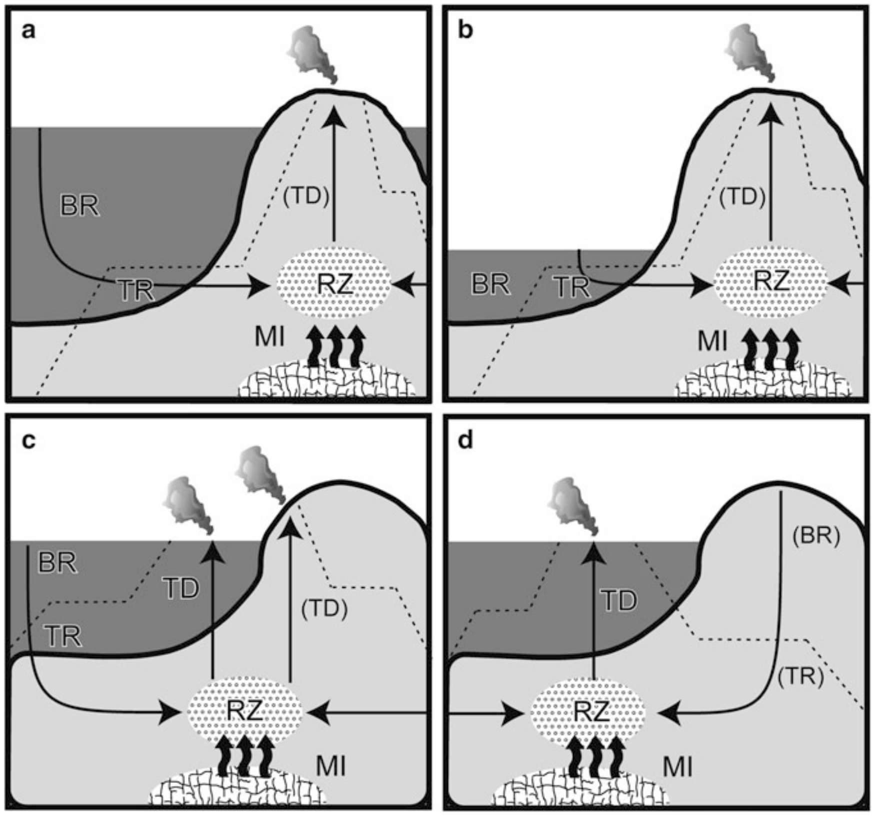

Fig. 30.8 Schematic illustrations of the 2D model representing methane origins based on the MMR model (after Kawagucci et al. (2011, 2013a) with minor modification). The geological setting and possible processes controlling fluid geochemistry, along with fluid circulation, are described (not to scale). *White*, *dark-gray*, and *light-gray fields* represent the seawater column, seafloor sediment, and rock basement, respectively. *Arrows* represent hydrothermal fluid migration paths. The two character designations represent the following: *BR* biological processes during the Recharge stage, *TR* thermal fluid-sediment interaction during the Recharge stage, *MI* magmatic volatile Inputs, *RZ* reaction zone, and *TR* thermal fluid-sediment interaction during the Discharge stage. *Dashed lines* are conceptual isotherms indicating the boundary between the microbial activity-dominated region and the thermochemical reaction-dominated region. Panels correspond to the models for describing (**a**) Iheya North and Hatoma, (**b**) Minami-Ensei, (**c**) Jade and Hakurei, and (**d**) Daiyon-Yonaguni

concentrations (~0.2 mM) (Kawagucci et al. 2011, 2013b). The low $\delta^{13}C_{CH4}$ values strongly suggest biogenic CH_4 as the dominant geochemical origin. The high C_1/C_{2+} ratios and the low H_2 concentrations eliminate the possibility of thermal fluid-sediment interaction during the discharge stage. All these geochemical indications can be consistently explained by dominance of microbial methanogenesis in the recharge stage as the origin of hydrothermal fluid CH_4 (Kawagucci et al. 2011) (Fig. 30.8a). Carbon mass balance calculations for the Iheya North hydrothermal system, as well as subseafloor hydrogeological structures revealed by geophysical study (Tsuji et al. 2012), suggest that the recharge stage of the Iheya North hydrothermal system includes the spatially abundant OT-filling sediments surrounding the Iheya North Knoll. This requires more than several kilometers of subseafloor hydrothermal fluid migration from the OT-filling sediment to the NBC vent (Fig. 30.9a).

30.4.2 Minami-Ensei

The Minami-Ensei hydrothermal fluid features high $\delta^{13}C_{CH4}$ values (−25 ‰), high C_1/C_{2+} ratios (>1,710), nearly equilibrated δD_{CH4} values (−105 ‰), and low H_2 concentrations (0.04 mM) (Fig. 30.4) (Kawagucci et al. 2013a). The high $\delta^{13}C_{CH4}$ values strongly suggest predominance of thermogenic CH_4 as its geochemical origin while the low H_2 concentrations rule out thermal fluid-sediment interaction during the discharge stage. These geochemical indications can be explained by dominance of thermal fluid-sediment interaction occurring in the recharge stage and reaction zone of hydrothermal fluid circulation as the origin of hydrothermal fluid CH_4 (Kawagucci et al. 2013a) (Fig. 30.8b). Less biogenic CH_4 contribution in the Minami-Ensei fluid implies a laterally shrunken hydrothermal fluid circulation that minimizes incorporation of biogenic CH_4 from the OT-filling sediment. This model seems consistent with the large volcanic body of the Minami-Ensei Knoll (approximately 700 m in height and 5 km in radius) (Fig. 30.9b).

30.4.3 Izena Hall (Jade and Hakurei)

The Jade and Hakurei hydrothermal fluids are known to have identical fluid geochemistry, including moderate $\delta^{13}C$ values (−32 ‰) and the nearly equilibrated δD values (−113 ‰) (Table 30.1) (Ishibashi et al. 2014). However, there are significant differences in C_2H_6 concentrations (C_1/C_{2+} = 14,900 for Jade and C_1/C_{2+} = 2,730 for Hakurei) and H_2 concentrations (0.06 mM for Jade and 1.4 mM for Hakurei). The almost identical fluid geochemistry can be explained by the fact that the Jade and Hakurei fluids likely share a common fluid reservoir, which means that they share a common fluid circulation system for the recharge stage and reaction zones (Fig. 30.8c) (Ishibashi et al. 2014). This model does not conflict with the identical $\delta^{13}C_{CH4}$ and δD_{CH4} values at the case that the hydrothermal fluid CH_4 of these fields are mainly derived from the recharge stage of hydrothermal fluid circulation. The moderate $\delta^{13}C_{CH4}$ value suggests concomitant biogenic and thermogenic CH_4 in the recharge stage. In turn, the relatively low C_1/C_{2+} ratios (Fig. 30.7) and high H_2 concentrations of the Hakurei fluid (Fig. 30.4) suggest thermal fluid-sediment interaction during the discharge stage. Because the sedimentary settings of the discharge stages are quite different between the fields (thick sediment-covered Hakurei field and sediment-starved Jade field), it is reasonable that thermogenic hydrocarbons and molecular hydrogen entrained into the upwelling fluid occur only in the Hakurei field (Fig. 30.8c) (Kawagucci et al. 2010a; Ishibashi et al. 2014). Hydrothermal fluid reservoir underlying the southern part of the bottom and north-eastern inner wall of the Izena Hall imply that the fluid recharge occurs not only within the Izena Cauldron but also in the volcanic body of the Izena Hall and the OT-filling sediment surrounding the Izena Hall, >4 km from the vents (Fig. 30.9c).

30.4.4 Daiyon-Yonaguni

The Daiyon-Yonaguni hydrothermal fluids have high $\delta^{13}C$ values (−26 ‰) and high H_2 concentrations (0.8–5.5 mM), but no C_1/C_{2+} ratios or δD values have been reported (Konno et al. 2006). The millimolar levels of H_2 concentration, despite the most likely silicic rock-hosted hydrothermal system (Fig. 30.4), suggest thermal fluid-sediment interaction occurs in the discharge stage (Fig. 30.8d). This interpretation is consistent with the high $\delta^{13}C$ values that indicate that thermogenic CH_4 is the dominant CH_4 source. The geochemical origin of the hydrothermal fluid CH_4, particularly less biogenic CH_4, implies that the outcropping knolls surrounding the fluid venting area serve as the recharge zone of hydrothermal fluid circulation: Such fluid recharge reduces incorporation of biogenic CH_4 from the sediment surrounding the Daiyon-Yonaguni knoll (Fig. 30.8d). Seafloor sediment of the fluid venting area, a valley of the small knolls, hosts thermal fluid-sediment interaction during fluid upwelling, which increases H_2 in the fluid (Fig. 30.8d). Assuming the above model, the lateral extent of the hydrothermal fluid circulation is <4 km in radius from the vents (Fig. 30.9d).

30.4.5 Hatoma

The Hatoma hydrothermal fluids feature low $\delta^{13}C$ values (−50 ‰) (Saegusa et al. 2006) and low H_2 concentrations (0.3 mM) (Kawagucci et al. 2010b). Although no C_1/C_{2+} ratios or δD values have been reported, the geochemical origin of CH_4 in the Hatoma fluid can be explained by a model similar to that of the Iheya North field: Biogenic CH_4 is incorporated during the recharge stage of fluid circulation while there is little involvement of thermogenic compounds (Fig. 30.8a). Because the Hatoma Knoll is small (approximately 1 km in radius) compared with the other OT knolls hosting high-temperature hydrothermal fields (Fig. 30.9), the OT-filling sediments surrounding the Hatoma Knoll are likely the recharge stage for hydrothermal fluid circulation and the source of biogenic CH_4 in the vent fluid (Fig. 30.9e).

30.5 Concluding Remarks

This chapter provides a compilation of high-temperature hydrothermal fluid geochemistry from the OT hydrothermal fields. The generation of the 'TAIGA of Methane' (in other words, how and where fluid-sediment interaction occurs within a hydrothermal system) is classified by the geochemical and geographical origins of the venting methane into three patterns: (1) microbial methanogenesis in the sedimentary environment during the recharge stage, (2) thermal degradation of sedimentary organic matter during the recharge stage, and (3) thermal degradation of sedimentary organic matter during high-temperature hydrothermal fluid upwelling through the sediment layer beneath the vent (Fig. 30.8). The discussion of the origins of CH_4 provides implications for the lateral extents of hydrothermal fluid circulation in each OT field (Fig. 30.9), such as larger contribution of biogenic CH_4 relating to more widespread recharge zone. However, this remains highly speculative. To strengthen the model, an understanding of subseafloor hydrogeological conditions via analysis of seismic reflection

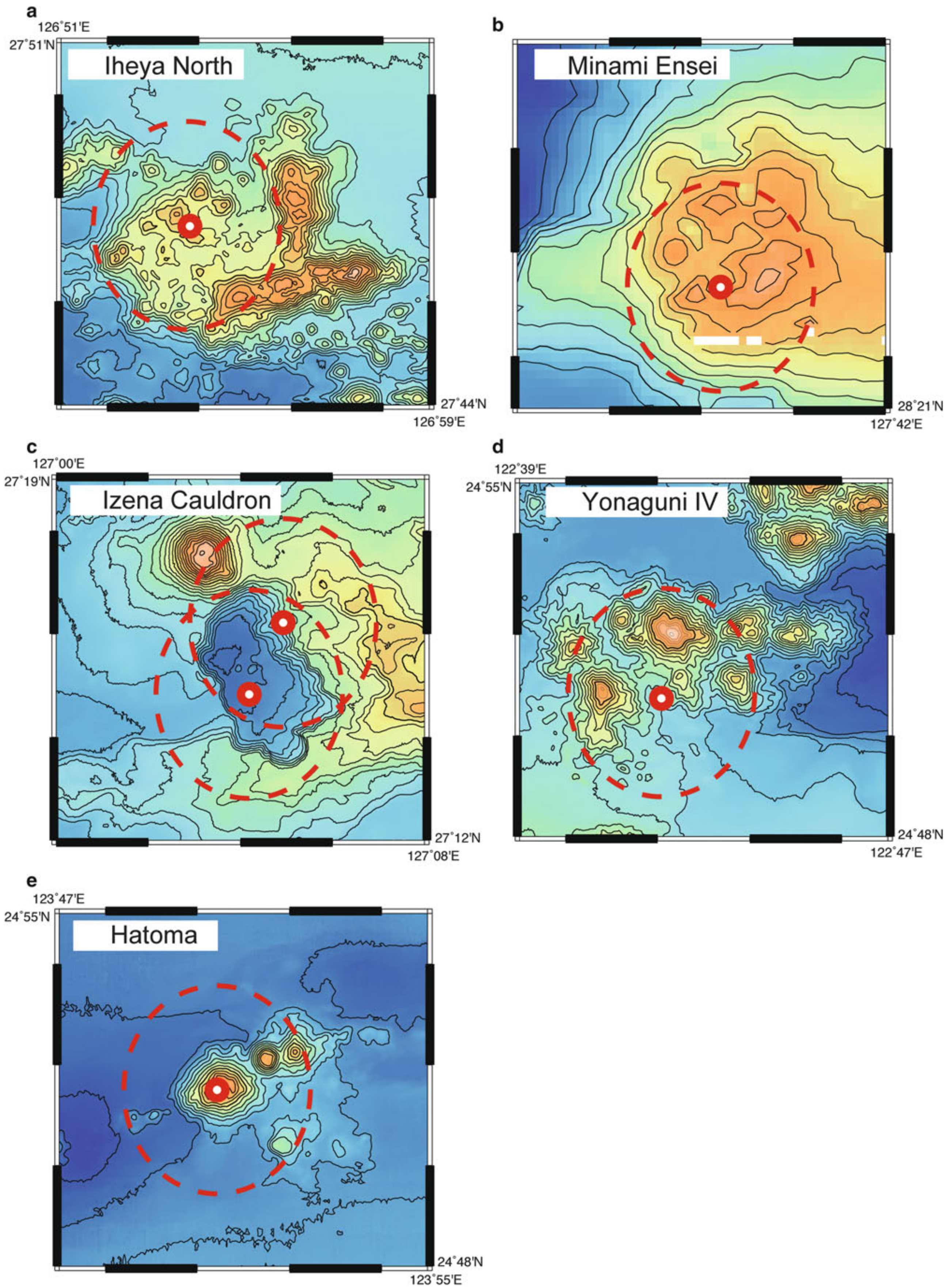

Fig. 30.9 Bathymetry maps of the six high-temperature hydrothermal fields at the same horizontal scale (coloring of depths is independent among the maps). *Broken red circles* on the maps represent the 2-miles radius from the main vent for each hydrothermal field

data and measurement of the permeability of cored rocks from seafloor drilling is essential. Nevertheless, the multiple geochemical tracer approach, when combined with interdisciplinary geological and microbiological investigations, will be a great breakthrough in clarifying the geochemical and geographical origins of CH_4 and associated hydrocarbons not only in deep-sea hydrothermal systems but also in the other sub(sea)floor geofluid systems, including subseafloor methane hydrate.

Acknowledgements I appreciate Ken Takai and the members of the TAIGA project for their valuable collaboration in studying deep-sea hydrothermal activity in the Okinawa Trough.

References

Bischoff JL, Rosenbauer RJ (1984) The critical-point and 2-phase boundary of seawater, 200–500°˜C. Earth Planet Sci Lett 68 (1):172–180

Butterfield DA, Mcduff RE, Mottl MJ, Lilley MD, Lupton JE, Massoth GJ (1994) Gradients in the composition of hydrothermal fluids from the endeavor segment vent field – phase-separation and brine loss. J Geophys Res Solid Earth 99(B5):9561–9583

Butterfield DA, Seyfried WE Jr, Lilley MD (2003) Composition and evolution of hydrothermal fluids. In: Halbach PE, Tunnicliffe V, Hein JR (eds) Energy and mass transfer in marine hydrothermal systems. Dahlem University Press, Germany, pp 124–161

Butterfield DA et al (2004) Mixing, reaction and microbial activity in the sub-seafloor revealed by temporal and spatial variation in diffuse flow vents at axial volcano. In: Wilcock WSD, Delong EF, Kelley DS, Baross JA, Cary CS (eds) The subseafloor biosphere at mid-ocean ridges. AGU, Washington, DC, pp 269–289

Charlou JL, Donval JP, Douville E, Jean-Baptiste P, Radford-Knoery J, Fouquet Y, Dapoigny A, Stievenard M (2000) Compared geochemical signatures and the evolution of menez Gwen (37°50′N) and lucky strike (37°17′N) hydrothermal fluids, south of the Azores triple junction on the Mid-Atlantic ridge. Chem Geol 171 (1–2):49–75

Charlou JL, Donval JP, Konn C, Ondréas H, Fouquet Y, Jean-Baptiste P, Fourré E (2010) High production and fluxes of H_2 and CH_4 and evidence of abiotic hydrocarbon synthesis by serpentinization in ultramafic-hosted hydrothermal systems on the Mid-Atlantic Ridge. In: Rona PA, Devey CW, Dyment J, Murton BJ (eds) Diversity of hydrothermal systems on slow spreading ocean ridges, vol 188, Geophysics monograph series. AGU, Washington, DC, pp 265–296

Chiba H et al (1993) Hydrothermal activity at the Minami-Ensei Knoll. Okinawa Trough: chemical characteristics of hydrothermal solutions. JAMSTECTR Deep Sea Res 9:271–282 (in Japanese with English abstract)

de Ronde CEL et al (2011) Submarine hydrothermal activity and gold-rich mineralization at Brother Volcano, Kermadec Arc, New Zealand. Miner Deposita. doi:10.1007/s00126-00011-00345-00128

Feisthauer S, Vogt C, Modrzynski J, Szlenkier M, Kruger M, Siegert M, Richnow HH (2011) Different types of methane monooxygenases produce similar carbon and hydrogen isotope fractionation patterns during methane oxidation. Geochim Cosmochim Acta 75 (5):1173–1184

Fouquet Y et al (2010) Geodiversity of hydrothermal processes along the Mid-Atlantic Ridge and ultramafic-hosted mineralization: a new type of oceanic Cu-Zn-Co-Au volcanogenic massive sulfide deposit. In: Rona PA, Devey CW, Dyment J, Murton BJ (eds) Diversity of hydrothermal systems on slow spreading ocean ridges, vol 188, Geophysics monograph series. AGU, Washington, DC, pp 321–368

Gallant RM, Von Damm KL (2006) Geochemical controls on hydrothermal fluids from the Kairei and Edmond Vent Fields, 23°-25°˜S, Central Indian Ridge. Geochem Geophys Geosyst 7

Gamo T (1995) Wide variation of chemical characteristics of submarine hydrothermal fluids due to the secondary modification processes after high temperature water-rock interaction: a review. In: Sakai H, Nozaki Y (eds) Biogeocheimical processes and ocean flux in the western pacific. Terra Scientific Publishing Company (TERRAPUB), Tokyo, pp 425–451

Gamo T, Sakai H, Kim ES, Shitashima K, Ishibashi J (1991) High alkalinity Due to sulfate reduction in the clam hydrothermal field, Okinawa Trough. Earth Planet Sci Lett 107(2):328–338

Gamo T, Okamura K, Charlou JL, Urabe T, Auzende JM, Ishibashi J, Shitashima K, Chiba H, Shipboard Scientific Party (1997) Acidic and sulfate-rich hydrothermal fluids from the Manus back-arc basin, Papua New Guinea. Geology 25:139–142

Gamo T et al (2001) Chemical characteristics of newly discovered black smoker fluids and associated hydrothermal plumes at the Rodriguez Triple Junction, Central Indian Ridge. Earth Planet Sci Lett 193(3–4):371–379

German CR, Von Damm KL (2003) 6.07 – hydrothermal processes. In: Heinrich DH, Karl KT (eds) Treatise on geochemistry. Pergamon, Oxford, pp 181–222

Gieskes JM, Simoneit BRT, Goodfellow WD, Baker PA, Mahn C (2002) Hydrothermal geochemistry of sediments and pore waters in Escanaba Trough – ODP Leg 169. Appl Geochem 17 (11):1435–1456

Gilbert A, Yamada K, Yoshida N (2013) Exploration of intramolecular ^{13}C isotope distribution in long chain n-alkanes (C11–C31) using isotopic ^{13}C NMR. Org Geochem 62:56–61

Grimaud D, Ishibashi J, Lagabrielle Y, Auzende JM, Urabe T (1991) Chemistry of hydrothermal fluids from the 17°˜S active-site on the north Fiji basin ridge (Sw pacific). Chem Geol 93(3–4):209–218

Hirose T, Kawagucci S, Suzuki K (2011) Mechanoradical H_2 generation during simulated faulting: implications for an earthquake-driven subsurface biosphere. Geophys Res Lett 38:L17303. doi:10.1029/2011GL048850

Hoefs J (2009) Stable isotope geochemistry, 6th edn. Springer, Berlin, p 285

Hongo Y, Obata H, Gamo T, Nakaseama M, Ishibashi J, Konno U, Saegusa S, Ohkubo S, Tsunogai U (2007) Rare earth elements in the hydrothermal system at Okinawa Trough back-arc basin. Geochem J 41:1–15

Horita J, Berndt ME (1999) Abiogenic methane formation and isotopic fractionation under hydrothermal conditions. Science 285 (5430):1055–1057

Inagaki F et al (2006) Microbial community in a sediment-hosted CO_2 lake of the southern Okinawa Trough hydrothermal system. Proc Natl Acad Sci U S A 103(38):14164–14169

Ishibashi JI, Wakita H, Nojiri Y, Grimaud D, Jeanbaptiste P, Gamo T, Auzende JM, Urabe T (1994a) Helium and carbon geochemistry of hydrothermal fluids from the north Fiji basin spreading ridge (southwest pacific). Earth Planet Sci Lett 128(3–4):183–197

Ishibashi J, Grimaud D, Nojiri Y, Auzende JM, Urabe T (1994b) Fluctuation of chemical-compositions of the phase-separated hydrothermal fluid from the North Fiji Basin Ridge. Mar Geol 116 (1–2):215–226

Ishibashi J, Sano Y, Wakita H, Gamo T, Tsutsumi M, Sakai H (1995) Helium and carbon geochemistry of hydrothermal fluids from the mid-Okinawa trough back-arc basin, southwest of Japan. Chem Geol 123(1–4):1–15

Ishibashi J, Sato M, Sano Y, Wakita H, Gamo T, Shanks WC (2002) Helium and carbon gas geochemistry of pore fluids from the sediment-rich hydrothermal system in Escanaba Trough. Appl Geochem 17(11):1457–1466

Ishibachi J et al (2002b) Concentration of biologically important chemical species in hydrothermal fluids from submarine arc volcano suiyo seamount. Eos Trans AGU 83(47), Fall Meets. Suppl., Abstract #V11C-05

Ishibashi J-I, Noguchi T, Toki T, Miyabe S, Yamagami S, Onishi Y, Yamanaka T, Yokoyama Y, Omori E, Takahashi Y, Hatada K, Nakaguchi Y, Yoshizaki M, Konno U, Shibuya T, Takai K, Inagaki F, Kawagucci S (2014) Diversity of fluid geochemistry affected by processes during fluid upwelling in active hydrothermal fields in the Izena Hole, the middle Okinawa Trough back-arc basin. Geochem J 48(3):357–369

Kawagucci S, Okamura K, Kiyota K, Tsunogai U, Sano Y, Tamaki K, Gamo T (2008) Methane, manganese, and helium-3 in newly discovered hydrothermal plumes over the Central Indian Ridge, 18°-20°˜S. Geochem Geophys Geosyst 9:Q10002. doi:10.1029/2008GC002082

Kawagucci S, Shirai K, Lan TF, Takahata N, Tsunogai U, Sano Y, Gamo T (2010a) Gas geochemical characteristics of hydrothermal plumes at the HAKUREI and JADE vent sites, the Izena Cauldron, Okinawa Trough. Geochem J 44(6):507–518

Kawagucci S, Toki T, Ishibashi J, Takai K, Ito M, Oomori T, Gamo T (2010b) Isotopic variation of molecular hydrogen in 20–375°˜C hydrothermal fluids as detected by a new analytical method. J Geophys Res Biogeosci 115, G03021. doi:10.1029/2009JG001203

Kawagucci S et al (2011) Hydrothermal fluid geochemistry at the Iheya North field in the mid-Okinawa Trough: implication for origin of methane in subseafloor fluid circulation systems. Geochem J 45 (2):109–124

Kawagucci S et al (2013a) Geochemical origin of hydrothermal fluid methane in sediment-associated fields and its relevance to the geographical distribution of whole hydrothermal circulation. Chem Geol 339:213–225

Kawagucci S et al (2013b) Post-drilling changes in fluid discharge pattern, mineral deposition, and fluid chemistry in the Iheya North hydrothermal field, Okinawa Trough. Geochem Geophys Geosyst 14:4774–4790

Kishida K, Sohrin Y, Okamura K, Ishibachi J (2004) Tungsten enriched in submarine hydrothermal fluids. Earth Planet Sci Lett 222 (3–4):819–827

Konno U, Tsunogai U, Nakagawa F, Nakaseama M, Ishibashi JI, Nunoura T, Nakamura KI (2006) Liquid CO_2 venting on the seafloor: Yonaguni knoll IV hydrothermal system, Okinawa Trough. Geophys Res Lett 33:L16607

Kumagai H et al (2008) Geological background of the Kairei and Edmond hydrothermal fields along the Central Indian Ridge: implications of their vent fluids' distinct chemistry. Geofluids 8 (4):239–251

Lilley MD, Butterfield DA, Olson EJ, Lupton JE, Macko SA, Mcduff RE (1993) Anomalous CH_4 and NH_4^+ concentrations at an unsedimented mid-ocean-ridge hydrothermal system. Nature 364 (6432):45–47

Lilley MD, Butterfield DA, Lupton JE, Olson EJ (2003) Magmatic events can produce rapid changes in hydrothermal vent chemistry. Nature 422(6934):878–881

Lin LH, Slater GF, Lollar BS, Lacrampe-Couloume G, Onstott TC (2005) The yield and isotopic composition of radiolytic H-2, a potential energy source for the deep subsurface biosphere. Geochim Cosmochim Acta 69(4):893–903

McCollom TM (2008) Observation, experimental, and theoretical constraints on carbon cycling in mid-ocean ridge hydrothermal systems. In: Lowell RP, Seewald JS, Metaxas A, Perfit MR (eds) Magma to microbe: modeling hydrothermal processes at ocean spreading centers. American Geophysical Union, Washington, DC, pp 193–213

McCollom TM (2013) Laboratory simulations of abiotic hydrocarbon formation in Earth's deep subsurface. Rev Min Geochem 75:467–494

McCollom TM, Seewald JS (2006) Carbon isotope composition of organic compounds produced by abiotic synthesis under hydrothermal conditions. Earth Planet Sci Lett 243(1–2):74–84

McCollom TM, Bach WG (2009) Thermodynamic constraints on hydrogen generation during serpentinization of ultramafic rocks. Geochim Cosmochim Acta 73(3):856–875

McCollom TM, Lollar BS, Lacrampe-Couloume G, Seewald JS (2010) The influence of carbon source on abiotic organic synthesis and carbon isotope fractionation under hydrothermal conditions. Geochim Cosmochim Acta 74(9):2717–2740

Merlivat L, Pineau F, Javoy M (1987) Hydrothermal vent waters at 13°˜N on the east pacific rise – isotopic composition and gas concentration. Earth Planet Sci Lett 84(1):100–108

Mottl MJ et al (2011) Chemistry of hot springs along the eastern Lau spreading center. Geochim Cosmochim Acta 75 (4):1013–1038

Nakagawa S, Takai K, Inagaki F, Chiba H, Ishibashi J, Kataoka S, Hirayama H, Nunoura T, Horikoshi K, Sako Y (2005) Variability in microbial community and venting chemistry in a sediment-hosted backarc hydrothermal system: Impacts of subseafloor phase-separation. FEMS Microbiol Ecol 54(1):141–155

Nakai N, Yoshida N, Ando N (1974) Isotopic studies on oil and gas fields in Japan. Chikyu Kagaku 7:87–98 (in Japanese with English abstract)

Nakano A, Matsumura M, Ishibashi J (2001) Geochemistry of hydrothermal fluids from the Hatoma Knoll in the South Okinawa Trough. JAMSTEC J Deep Sea Res 18:139–144

Noguchi T, Shinjo R, Ito M, Takada J, Oomori T (2011) Barite geochemistry from hydrothermal chimneys of the Okinawa Trough: insight into chimney formation and fluid/sediment interaction. J Mineral Petrol Sci 106(1):26–35

Pearson A, Seewald JS, Eglinton TI (2005) Bacterial incorporation of relict carbon in the hydrothermal environment of Guaymas Basin. Geochim Cosmochim Acta 69(23):5477–5486

Proskurowski G, Lilley MD, Brown TA (2004) Isotopic evidence of magmatism and seawater bicarbonate removal at the endeavour hydrothermal system. Earth Planet Sci Lett 225(1–2):53–61

Proskurowski G, Lilley MD, Kelley DS, Olson EJ (2006) Low temperature volatile production at the Lost City Hydrothermal Field, evidence from a hydrogen stable isotope geothermometer. Chem Geol 229(4):331–343

Reeves EP, Seewald JS, Saccocia P, Bach W, Craddock PR, Shanks WC, Sylva SP, Walsh E, Pichler T, Rosner M (2011) Geochemistry of hydrothermal fluids from the PACMANUS, Northeast Pual and Vienna Woods hydrothermal fields, Manus Basin, Papua New Guinea. Geochim Cosmochim Acta 75(4):1088–1123

Reeves EP, Seewald JS, Sylva SP (2012) Hydrogen isotope exchange between n-alkanes and water under hydrothermal conditions. Geochim Cosmochim Acta 77:582–599

Saegusa S, Tsunogai U, Nakagawa F, Kaneko S (2006) Development of a multibottle gas-tight fluid sampler WHATS II for Japanese submersibles/ROVs. Geofluids 6(3):234–240

Sakai H, Gamo T, Kim ES, Tsutsumi M, Tanaka T, Ishibashi J, Wakita H, Yamano M, Oomori T (1990a) Venting of carbon-dioxide rich fluid and hydrate formation in mid-Okinawa Trough Backarc Basin. Science 248(4959):1093–1096

Sakai H et al (1990b) Unique chemistry of the hydrothermal solution in the mid-Okinawa Trough Backarc Basin. Geophys Res Lett 17 (12):2133–2136

Sano Y, Fischer TP (2013) The analysis and interpretation of noble gases in modern hydrothermal systems. In: Burnard P (ed) The noble gases as geochemical tracers, advances in isotope geochemistry. Springer, Berlin/Heidelberg, pp 249–317

Seewald JS, Seyfried WE (1990) The effect of temperature on metal mobility in subseafloor hydrothermal systems – constraints from basalt alteration experiments. Earth Planet Sci Lett 101 (2–4):388–403

Seewald JS, Seyfried WE, Shanks WC (1994) Variations in the chemical and stable-isotope composition of carbon and sulfur species during organic-rich sediment alteration – an experimental and theoretical-study of hydrothermal activity at Guaymas Basin, Gulf of California. Geochim Cosmochim Acta 58(22):5065–5082

Seyfried WE, Seewald JS, Berndt ME, Ding K, Foustoukos DI (2003) Chemistry of hydrothermal vent fluids from the main Endeavour field, northern Juan de Fuca Ridge: geochemical controls in the aftermath of June 1999 seismic events. J Geophys Res Solid Earth 108(B9):2429

Shinjo R, Kato Y (2000) Geochemical constraints on the origin of bimodal magmatism at the Okinawa Trough, an incipient back-arc basin. Lithos 54:117–137

Sugimoto A, Wada E (1995) Hydrogen isotopic composition of bacterial methane – CO_2/H_2 reduction and acetate fermentation. Geochim Cosmochim Acta 59(7):1329–1337

Suzuki R, Ishibashi JI, Nakaseama M, Konno U, Tsunogai U, Gena K, Chiba H (2008) Diverse range of mineralization induced by phase separation of hydrothermal fluid: case study of the Yonaguni Knoll IV hydrothermal field in the Okinawa Trough back-arc basin. Res Geol 58(3):267–288

Takai K, Nakamura K, Toki T, Tsunogai U, Miyazaki M, Miyazaki J, Hirayama H, Nakagawa S, Nunoura T, Horikoshi K (2008) Cell proliferation at 122°˜C and isotopically heavy CH_4 production by a hyperthermophilic methanogen under high-pressure cultivation. Proc Natl Acad Sci U S A 105(31):10949–10954

Tivey MK, Stakes DS, Cook TL, Hannington MD, Petersen S (1999) A model for growth of steep-sided vent structures on the Endeavour Segment of the Juan de Fuca Ridge: results of a petrologic and geochemical study. J Geophys Res Solid Earth 104 (B10):22859–22883

Toki T, Tsunogai U, Ishibashi J, Utsumi M, Gamo T (2008) Methane enrichment in low-temperature hydrothermal fluids from the Suiyo Seamount in the Izu-Bonin Arc of the western Pacific Ocean. J Geophys Res Solid Earth 113:B08s13. doi:10.1029/2007jb005476

Tsuji T, Takai K, Oiwane H, Nakamura Y, Masaki Y, Kumagai H, Kinoshita M, Yamamoto F, Okano T, Kuramoto S (2012) Hydrothermal fluid flow system around the Iheya North Knoll in the mid-Okinawa trough based on seismic reflection data. J Volcanol Geoth Res 213:41–50

Tsunogai U, Ishibashi J, Wakita H, Gamo T, Watanabe K, Kajimura T, Kanayama S, Sakai H (1994) Peculiar features of Suiyo seamount hydrothermal fluids, Izu-Bonin arc – differences from subaerial volcanism. Earth Planet Sci Lett 126(4):289–301

Tsunogai U, Nakagawa F, Gamo T, Ishibashi J (2005) Stable isotopic compositions of methane and carbon monoxide in the Suiyo hydrothermal plume, Izu-Bonin arc: tracers for microbial consumption/production. Earth Planet Sci Lett 237(3–4):326–340

Valentine DL, Chidthaisong A, Rice A, Reeburgh WS, Tyler SC (2004) Carbon and hydrogen isotope fractionation by moderately thermophilic methanogens. Geochim Cosmochim Acta 68 (7):1571–1590

Von Damm KL, Lilley MD (2004) Diffuse flow hydrothermal fluids from 9°50′N east pacific rise: origin, evolution and biogeochemical controls. In: Wilcock WSD, Delong EF, Kelley DS, Baross JA, Cary CS (eds) The subseafloor biosphere at mid-ocean ridges. AGU, Washington, DC, pp 245–268

Von Damm KL, Edmond JM, Measures CI, Grant B (1985) Chemistry of submarine hydrothermal solutions at Guaymas Basin, Gulf of California. Geochim Cosmochim Acta 49(11):2221–2237

Von Damm KL, Parker CM, Zierenberg RA, Lilley MD, Olson EJ, Clague DA, McClain JS (2005) The Escanaba Trough, Gorda ridge hydrothermal system: temporal stability and subseafloor complexity. Geochim Cosmochim Acta 69(21):4971–4984

Welhan JA, Lupton JE (1987) Light hydrocarbon gases in Guaymas Basin hydrothermal fluids: thermogenic versus abiogenic origin. Am Assoc Petrol Geol Bull 71:215–223

Whiticar MJ (1999) Carbon and hydrogen isotope systematics of bacterial formation and oxidation of methane. Chem Geol 161 (1–3):291–314

Yanagawa K et al (2013) Metabolically active microbial communities in marine sediment under high-CO_2 and low-pH extremes. ISME J 7 (3):555–567

You CF, Butterfield DA, Spivack AJ, Gieskes JM, Gamo T, Campbell AJ (1994) Boron and Halide systematics in submarine hydrothermal systems – effects of phase-separation and sedimentary contributions. Earth Planet Sci Lett 123(1–4):227–238